Supporting Information

Synergistic Effect of Cobalt Boride Nanoparticles on MoS_2 Nanoflowers for Highly Efficient Hydrogen Evolution in Alkaline Media

Jie Lao[a], Dong Li[a], Chunli Jiang[a,b], Chunhua Luo[a,], Ruijuan Qi[a], Hechun Lin[a], Rong Huang[a,b], Geoffrey I. N. Waterhouse[c] and Hui Peng[a,b,*]*

[a] Key Laboratory of Polar Materials and Devices (MOE), Department of Electronics, East China Normal University, Shanghai, 200241, China.

[b] Collaborative Innovation Center of Extreme Optics, Shanxi University, Taiyuan, Shanxi 030006, China

[c] School of Chemical Sciences, The University of Auckland, Auckland 1142, New Zealand

*** Corresponding authors at:** Key Laboratory of Polar Materials and Devices (MOE), Department of Electronics, East China Normal University, Shanghai, 200241, China.

Address correspondence to: chluo@ee.ecnu.edu.cn, hpeng@ee.ecnu.edu.cn

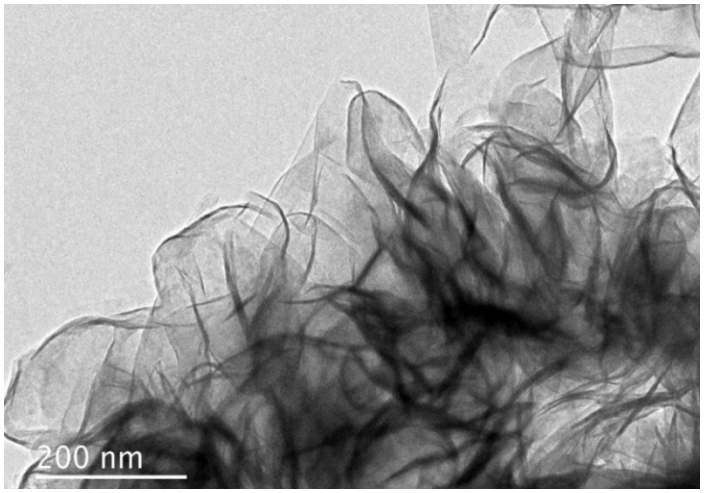

Figure S1. TEM image of the MoS_2 NFs.

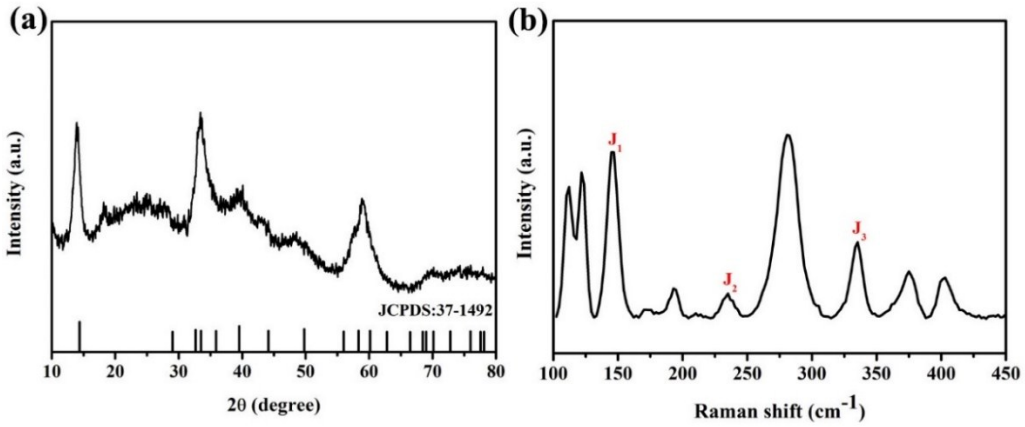

Figure S2. (a) XRD pattern and (b) Raman spectrum for the MoS_2 NFs.

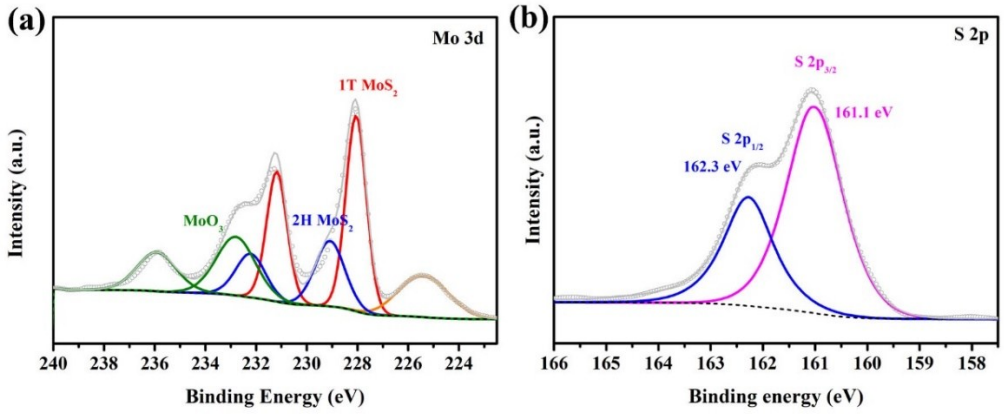

Figure S3. High resolution XPS spectra for the MoS_2 NFs: (a) Mo 3d region and (b) S 2p region.

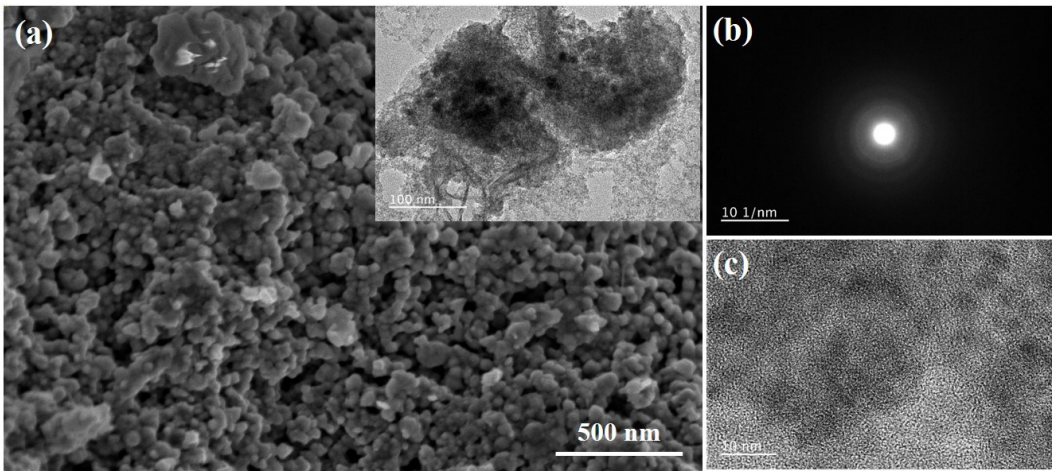

Figure S4. Morphological characterization of the CoB NPs. (a) SEM&TEM (inset) image, (b) SAED pattern, and (c) HRTEM image.

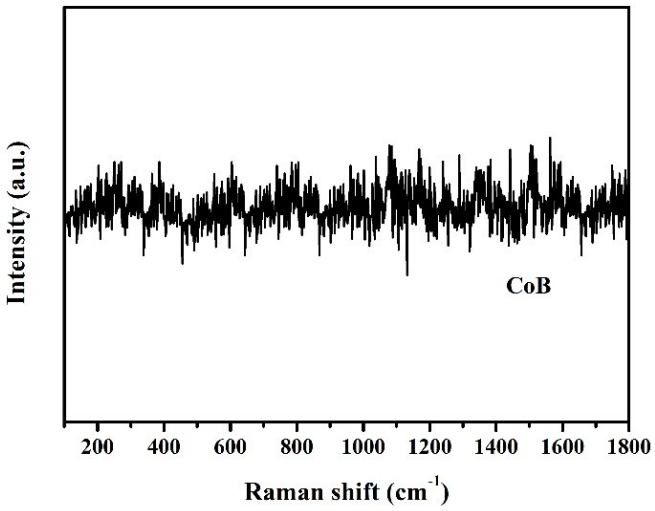

Figure S5. Raman spectrum of the CoB NPs.

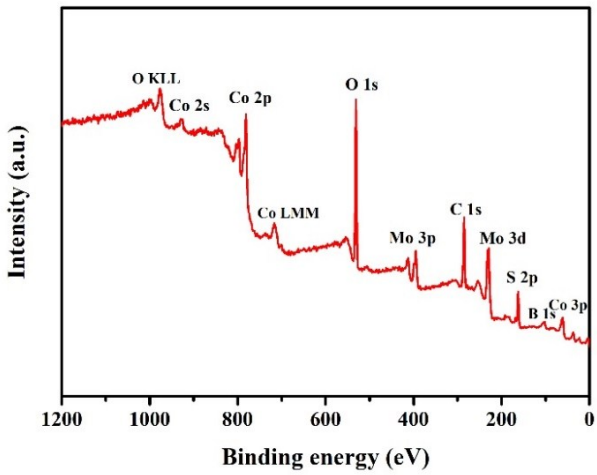

Figure S6. XPS survey spectrum for the CoB@MoS_2-0.5-300 hybrid.

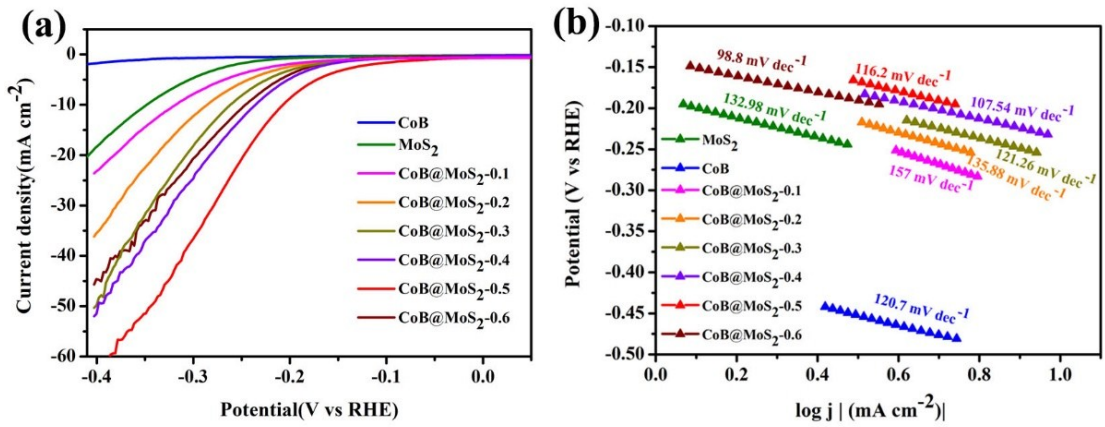

Figure S7. HER performance of various CoB@MoS_2-*x* hybrids (before annealing) in 1.0 M KOH. (a) Polarization curves, and (b) Tafel plots.

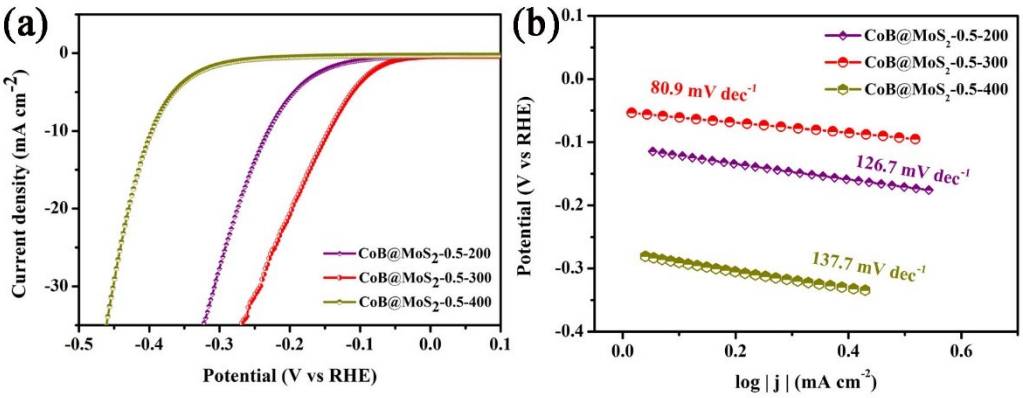

Figure S8. Polarization curves (a) and corresponding Tafel slopes (b) for the CoB@MoS_2-*x*-*y* hybrids (after annealing at different temperatures) in 1.0 M KOH.

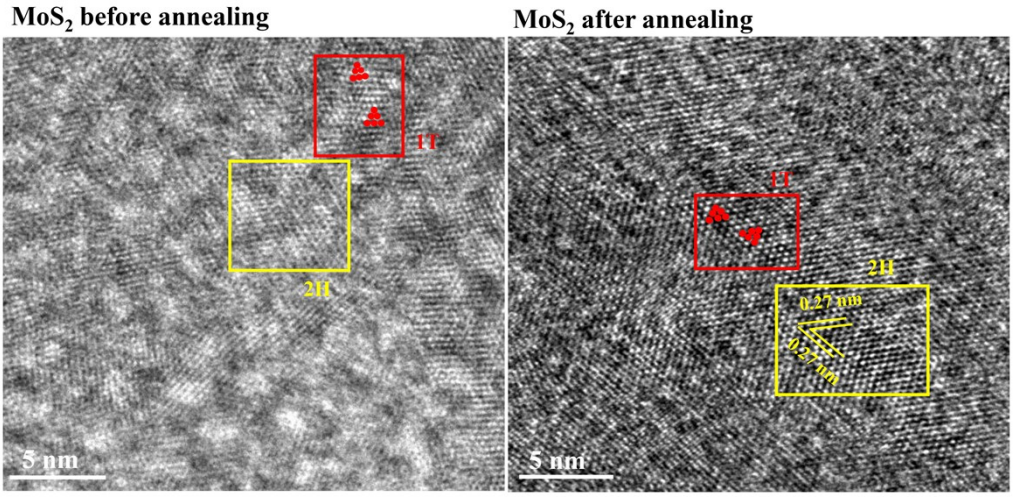

Figure S9. The HRTEM of MoS_2 before and after annealing. After the annealing, the lattice fringes became more obvious.

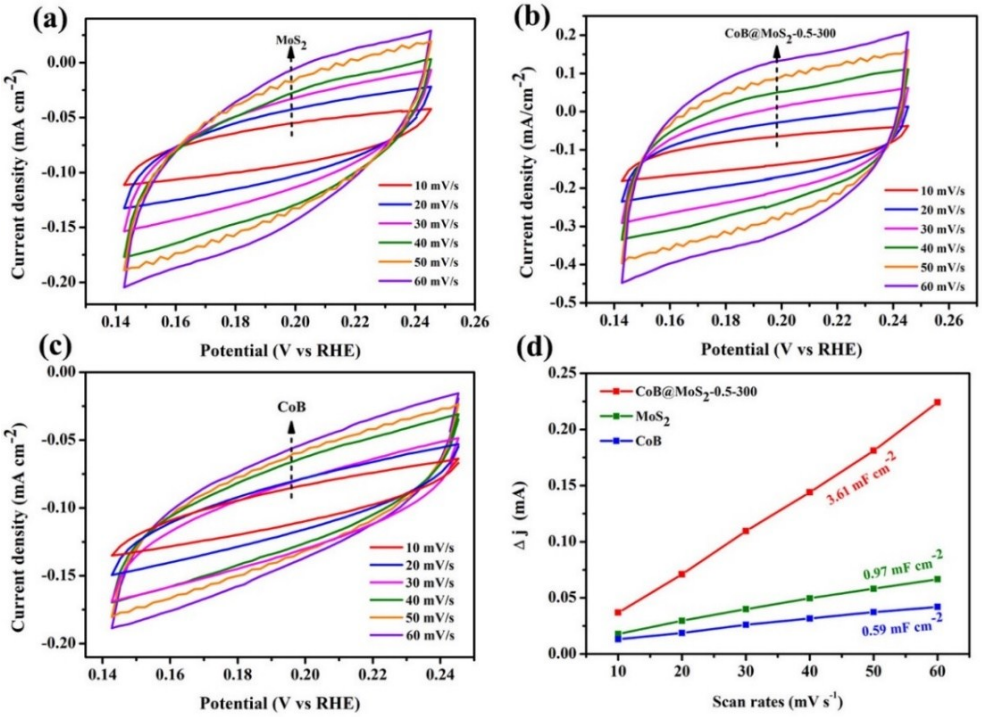

Figure S10. Cyclic voltammograms recorded at different scan rates in the non-Faradaic potential region (0.14-0.24 V vs. RHE) for (a) MoS_2, (b) CoB@MoS_2-0.5-300 and (c) CoB. (d) linear regression analyses used to estimate the double-layer area capacitances of MoS_2, CoB@MoS_2-0.5-300 and CoB.

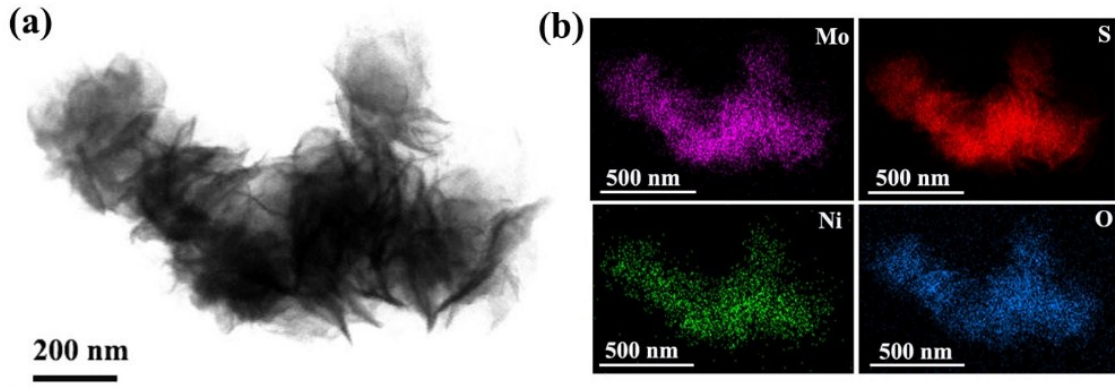

Figure S11. Morphological characterization of NiB@MoS_2-0.5-300 NFs. (a) TEM image, and (b) EDX element mapping images.

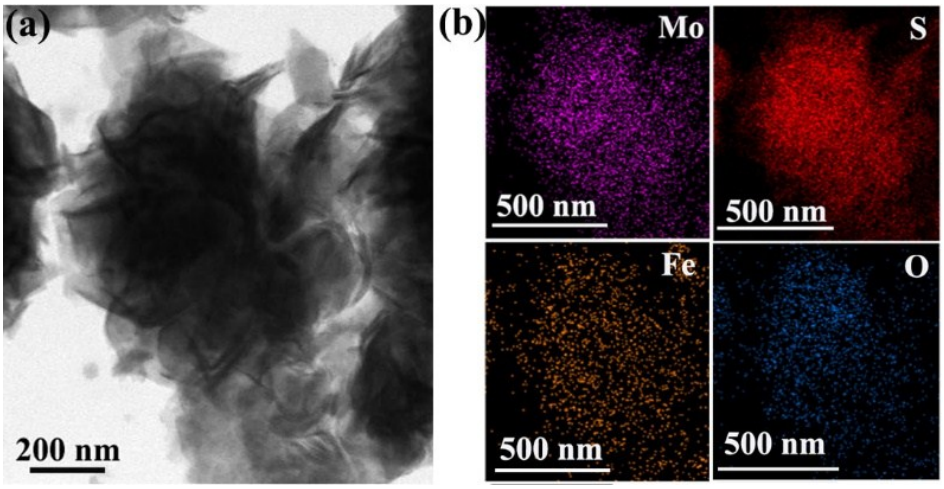

Figure S12. Morphological characterization of FeB@MoS_2-0.5-300 NFs. (a) TEM image, and (b) EDX element mapping images.

Table S1 HER performance of CoB@MoS_2-0.5 hybrid after annealing at different temperature under N_2

Catalysis	Overpotential at 10 mA cm^{-2}	Tafel Slope
CoB@MoS_2-0.5-200	232 mV	126.7 mV dec^{-1}
CoB@MoS_2-0.5-300	146 mV	80.9 mV dec^{-1}
CoB@MoS_2-0.5-400	398 mV	137.7 mV dec^{-1}

Table S2. HER performance of different MoS_2-based electrocatalysts in 1.0 M KOH

Catalyst	Overpotential (10 mA cm^{-2})	Tafel slope (mV dec^{-1})	Reference
$Ni(OH)_2$ /MoS_2	227 mV	105	*Nanoscale* 2018, 10, 19074.
$NiCo_2S_4$@MoS_2	194 mV	68	*New J. Chem*. 2019, 43, 3601
2D-MoS_2/$Ni(OH)_2$	185 mV	73	*Adv. Mater.* 2018, 30, 1801171.
Co-BDC/MoS_2	155 mV	86	*Small* 2019, 15, 1805511.
CoB-300	328 mV	136.2	Adv. Energy Mater. 2016, 6, 1502313.
Co_2B/Co/N−B−C/B_4C	220 mV	205	ACS Appl. Mater. Interfaces 2018, 10, 37067-37078
NiCoFeB	345 mV	98	Small 2019, 15, 1804212
NiCoB	363 mV	102	Small 2019, 15, 1804212
CoB@MoS_2-0.5-300	**146 mV**	**80.9**	**This work**